C-H Bond Activation

Transition-Metal Complexes with Sterically Demanding Ligands: Facile Thermal Intermolecular C–H Bond Activation in a Square-Planar Ir^{I} Complex**

*Stefan Nückel and Peter Burger**

Dedicated to Professor Robert G. Bergman on the occasion of his 60th birthday

The intermolecular activation of C–H bonds is a highly desirable process[1–8] and is part of many catalytic systems,[9–11] for example, the dehydrogenation of alkanes to alkenes.[12–14] Detailed studies by various groups clearly established that the C–H activation process is under kinetic rather than thermodynamic control in most cases.[12,13] Thus, highly reactive species, such as photochemically generated short-lived transients, for example, [Cp*Ir(PMe$_3$)] (Cp* = C_5Me_5), are often required,[3,15] while thermally initiated C–H activation processes under mild conditions are less common.[2,4,16] Herein, we describe a novel square-planar iridium(I) system **1**, which undergoes facile thermal *intermolecular* C–H activation in benzene at ambient temperature [Eq. (1)]. The observed

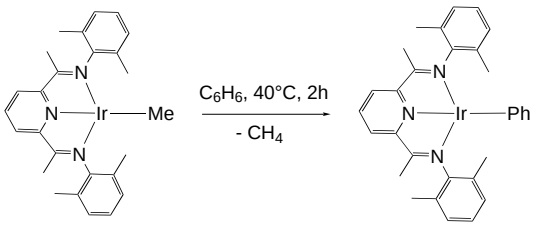

1 **2**

quantitative (1)

unusual low barrier is analyzed and traced by DFT methods providing guidelines for the design of novel systems, which would allow the activation of methane under mild conditions.

We have recently reported the synthesis of the iridium complex **1** and its rhodium analogue.[1] In the course of this study, we noticed facile intermolecular C–H activation in benzene leading quantitatively to the phenyl complex **2** and methane [Eq. (1)]. In the analogous reaction of **1** with C_6D_6 formation of [D_5]phenyl analogue of **2** and [D_1]methyl was observed. Both **1** and **2** could be characterized unambiguously

[*] Dr. P. Burger, Dr. S. Nückel
Anorg.-chem. Institut
Universität Zürich
Winterthurerstrasse 190, 8057 Zürich (Switzerland)
Fax: (+41) 1-635-6802
E-mail: chburger@aci.unizh.ch

[**] Part IV. We would like to thank the Swiss National Science Foundation for financial support. We are indebted to Prof. Heinz Berke for his generous support. For Part III see ref. [1].

  DOI: 10.1002/ange.200219908

as square-planar complexes by their X-ray crystal structures (Figure 1).[17] Compound **2** was also obtained by independent synthesis from the corresponding methoxy complex[1] and phenylmagnesium chloride in 38% yield.

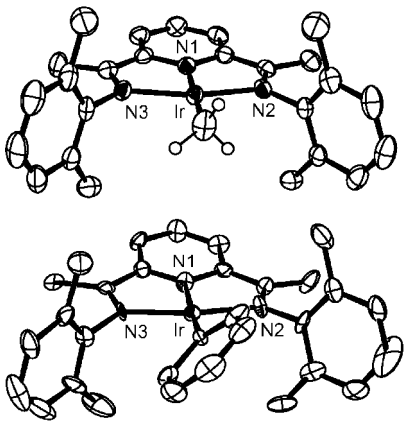

Figure 1. ORTEP plots (thermal elipsoids set at 50% probability) of complexes **1** (top) and **2** (bottom).

Monitoring the C–H activation process shown in Equation (1) by ^{1}H NMR spectroscopy indicated a clean conversion from **1**→**2** without detectable traces of intermediates. In neat [D_6]benzene under pseudo first-order conditions, a first-order decay of the starting material **1** with a free enthalpy of activation, $\Delta G_{313} = 23$ kcal mol^{-1} was measured.

Overall, the outcome of the C–H activation reaction resembles a σ-bond metathesis process, which is the anticipated mechanism for d^0 early-transition-metal and lanthanide row complexes.[8,18,19] For d^n-configured complexes with $n \geq 2$ there are other mechanistic alternatives, for example, a C–H oxidative-addition step, followed by C–H reductive elimination.[4,20,21] Investigations of late-transition-metal systems of which the cationic Ir^{III} compounds [Cp*Ir(PMe_3)Me]$^+X^-$ are prominent examples,[16,22] indicate that the two-step pathway is followed for these systems. However, it is extraordinary difficult to distinguish between these two mechanistic scenarios in the absence of experimental evidence for a C–H oxidative intermediate.[2,4,20,21,23] In the aforementioned Ir^{III} system, support for the two-step pathway was provided by DFT calculations prior to the recent isolation of a related Ir^V Si–H and C–H oxidative-addition product.[20,21]

To elucidate mechanistic details of the C–H activation system in the square-planar complex **1**, we also resorted to DFT methods. Since steric factors were deemed to play a crucial role in the C–H activation process, DFT calculations were performed on the full system. The efficient parallel RI-DFT implementation[24,25] (BP-86 functional; basis: TZVP, ECP-60-MWB (Ir), SVP (C,H,N)) of the Turbomole program package[26] allowed the use of a pure quantum-mechanical approach rather than the potentially less reliable quantum mechanical/molecular modeling methods,[27,28] which have been applied by other groups for systems of related size.

Although we did not intend to prejudge the mechanism, after considering the d^8-configuration of **1** we preferred the notion of the two-step mechanism. Preliminary experimental evidence for an Ir^{III} intermediate was provided by the reaction of **1** with H_2, which led to a tentatively assigned, trihydride Ir^{III} complex and methane.[29] The two-step view was partially supported by the absence of a transition state for the σ-bond metathesis pathway in our DFT calculations. Furthermore, we considered C–H bond activation at a three-coordinate metal center, with C–H activation in benzene by [Ir($P i Pr_3$)$_2$Cl] being a well-established example.[30] Related results were recently reported for an iridium cycloalkane-dehydrogenation catalyst bearing a terdentate cyclometalated bisphosphane donor (PCP pincer ligand).[13] Considering the rigid chelating ligand in **1**, the cleavage of one of the nitrogen donor arms from the metal center was deemed to be inconsistent with the observed low activation energy. This idea was supported by the DFT calculations, which revealed an Ir–$N_{diimine}$ bond-dissociation enthalpy of 35 kcal mol^{-1}.

These results suggested that an alternative mechanistic scenario was operative; we have therefore studied the two-step mechanism starting from the square-planar complex **1**. For this pathway, we were able to identify the required transition states TS_{OA} and TS_{RE} and the C–H oxidative Ir^{III} intermediate I_{OA} (OA = oxidative addition, RE = reductive elimination) as stationary points[31] (Figure 2).

The calculated barrier of 22 kcal mol^{-1} leading from **1** via the square-pyramidal transition state TS_{OA} to the octahedral H_5C_6–H (with benzene) oxidative-addition product I_{OA} is in excellent agreement with the observed experimental value. It is noteworthy that the Ir^{III} intermediate, I_{OA}, is energetically "uphill" (+10 kcal mol^{-1}) from **1** and benzene. This readily explains the calculated low barrier of 12 kcal mol^{-1} for the reductive elimination of CH_4 passing over TS_{RE} to give the energetically favored final products **2** and methane (−4 kcal mol^{-1}). For the corresponding Rh system, $\mathbf{1_{Rh}}$, we calculated a significantly higher barrier of 27 kcal mol^{-1}, which is consistent with the observed reluctance of $\mathbf{1_{Rh}}$ to undergo C–H activation in benzene even at elevated temperatures.

The results of the DFT calculations for C–H activation in methane by complex **1** are also included in Figure 2. In accordance with previous studies,[2,3] the barrier is higher (by +6 kcal mol^{-1}) than for the C–H activation process in benzene. For the analogous less crowded, $\mathbf{1_{H4}}$ (Figure 2) however, we derived a substantially smaller barrier of just 19 kcal mol^{-1} for the C–H oxidative-addition step in methane (Figure 2). Using a value of 9 kcal mol^{-1} for the $T\Delta S^{\neq}$ term ($\Delta S^{\neq} = +30$ cal mol^{-1} K^{-1}) at RT, a free enthalpy of activation of $\Delta G^{\neq} \approx 28$ kcal mol^{-1} is estimated. This result suggested that methane could be activated under relatively mild thermal conditions in the $\mathbf{1_{H4}}$ system.

To understand the unprecedented low barriers for the C–H oxidative-addition process in the square-planar systems **1** and $\mathbf{1_{H4}}$,[32] we performed an intrinsic reaction coordinate (IRC) calculation [33] starting from the square-pyramidal (Figure 2) transition state TS_{OA} for the methane oxidative-addition step in $\mathbf{1_{H4}}$. In the forward direction, this led to the anticipated octahedral Ir^{III} product $\mathbf{I_{H4,CH4}}$. Following the backward reaction mode, the anticipated lengthening of the Ir–H and Ir–C and shortening of the C–H bond was

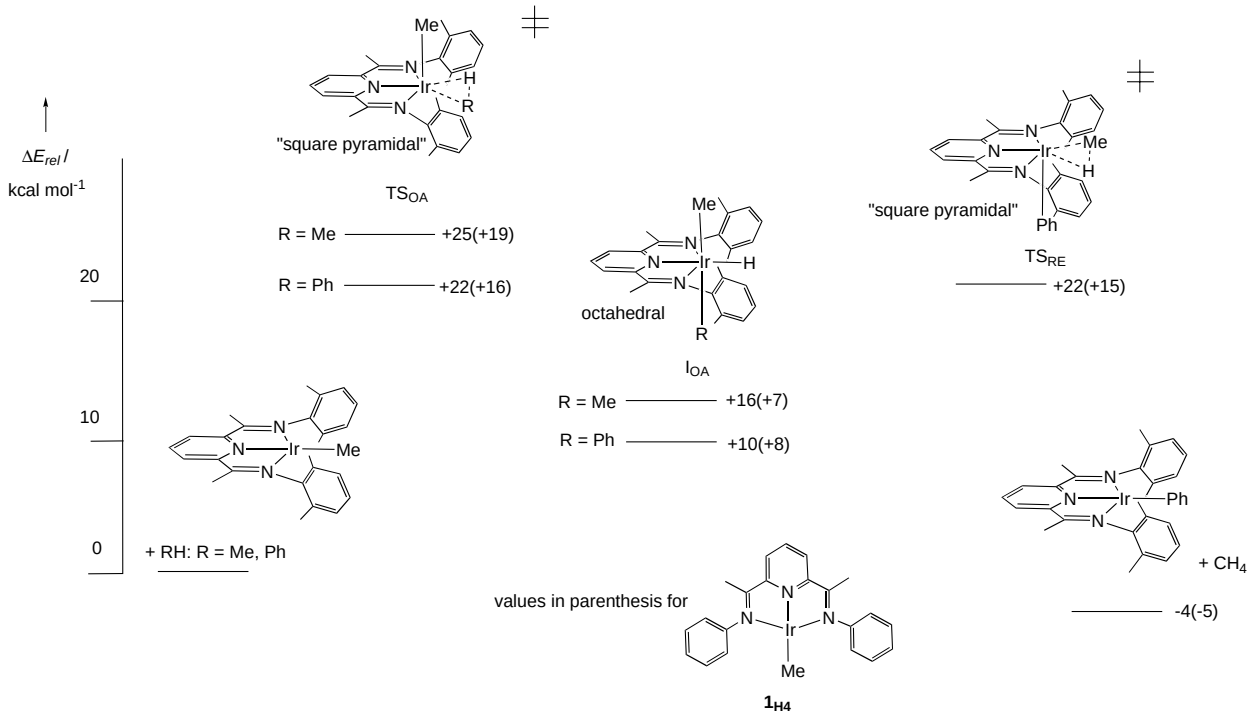

Figure 2. Energy diagram and proposed intermediates and transition states for the C–H activation process shown in Equation (1) based on DFT theory.

observed. More importantly, substantial opening of the $N_{pyridyl}$-Ir-Me angle from approximately 90° in the transition state was noticeable, and significant bending was still observed after methane was essentially fully released ($d(\mathrm{Ir}\cdots\mathrm{H}-\mathrm{CH_3}) = 2.5$ Å). This result clearly indicated bending of the methyl group away from the chelating-ligand–metal plane in the Ir complex as a crucial part of the C–H activation process and prompted us to calculate a Walsh diagram for this out-of-plane bending in complex **1** (Figure 3).

The small energy required for out-of-plane bending of the methyl group in complex **1** is noteworthy, approximately 12 kcal mol^{-1} for $\alpha = 70°$. For the unsubstituted model compound [{2,6-[C(CH$_3$)=NH]$_2$pyridine}IrMe] (**1$_{model}$**) we noticed an even more shallow potential for the bending process, with the Walsh diagrams of **1$_{model}$** and **1$_{H4}$** being essentially superimposable (Figure 3). Since identical kinetic and thermodynamic data for the methane C–H oxidative activation process were also derived for **1$_{model}$** and **1$_{H4}$**, we anticipate that the lower barriers in the N-phenyl substituted complex **1$_{H4}$** (compared to **1**) can be attributed to the more shallow potential of the bending process, which is a consequence of the reduced steric crowding. This situation is in contrast to the Walsh diagram obtained for this process in the tridentate phosphorus donor complex, [{κ^3-MePCH$_2$CH$_2$PMe$_2$)$_2$}IrMe]. For the latter, a significantly steeper potential for the bending process is observed and therefore a substantially larger contribution to the activation energy is anticipated. Before the origin of the difference between the N and P ligands will be addressed, the electronic structure of the bent species will be discussed.

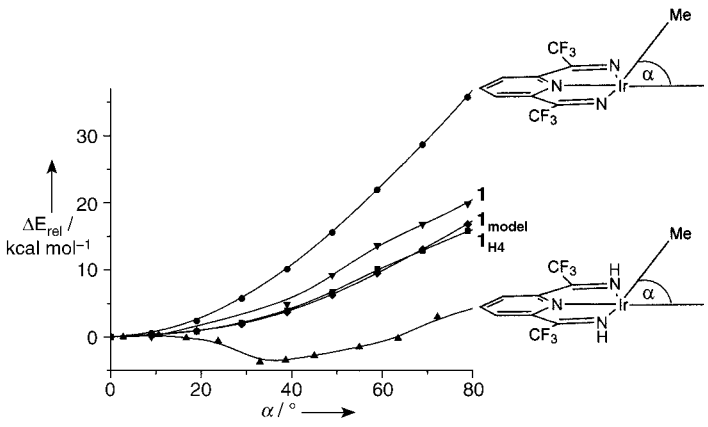

Figure 3. Walsh diagram for out-of-plane bending of [{κ^3-MeP(CH$_2$CH$_2$PMe$_2$)$_2$}IrMe] (●), complex **1** (▼), **1$_{model}$** (◆), **1$_{H4}$** (■), and [{2,6-[C(CF$_3$)=NH]$_2$-pyridine}IrMe] (▲).

As previously analyzed in EHT and DFT studies, an out-of-plane bending distortion of one ligand in a d^8-configured square-planar ML$_4$ complex leads to a C_{2v}-symmetrical ML$_4$ species which is isolobal to the methylene carbene unit, CH$_2$.[34,35] The [Fe(CO)$_4$] singlet state is a prominent representative of this type of compound. In the bent complex **1**, this is also nicely reflected in the frontier orbitals ($\alpha = 90°$) which have the required π(HOMO) and σ(LUMO) symmetry (Figure 4). Small C–H activation barriers would therefore be expected for this type of species. It should be noted that for angles $\alpha < 90°$, a residual two-orbital four-electron repulsive term between a filled metal d orbital and the occupied σ CH orbital raises the barrier.[35] This term vanishes when a bending angle of 90° is attained, as observed in the transition state TS$_{OA}$ of complex **1**.

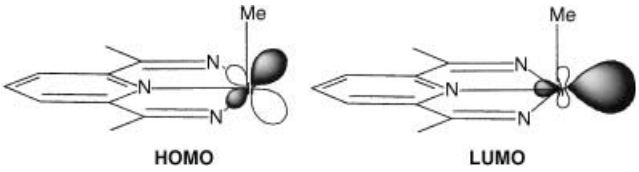

Figure 4. Frontier orbitals of complex **1**.

Out-of-plane bending potentials in d^8-configured square-planar ML_4 complexes have been discussed in the context of oxidative addition of H_2.[36,37] The major contribution to this unfavorable process arises from a two-orbital-four-electron repulsive interaction between the occupied metal-based d_{xz} orbital and the methyl σ orbitals upon bending, which is nonbonding in the undistorted square-planar ML_4 complex. As shown in Figure 5 this repulsive interaction is significantly lowered by mixing of a diimine, pyridine-ligand-based π-acceptor orbital in the iridium methyl complex **1**.

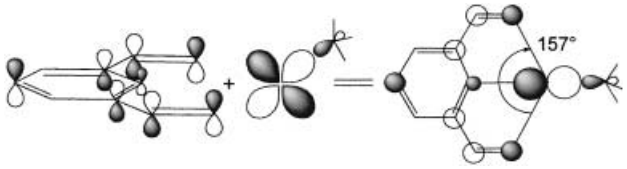

Figure 5. Lowering of the repulsive interaction between the metal d_{xz} and the methyl σ orbitals by mixing of a π-acceptor orbital in complex **1**.

The major stabilizing contribution stems from back donation into the -C=$N_{diimine}$ unit. It has to be emphasized that this interaction is nonbonding if the ligands are located in the nodal plane of the d_{xz} orbital. As can be readily seen from the $N_{diimine}$-Ir-$N_{diimine}$ angle of 157° in the X-ray crystal structure of **1,** the diimine N_{donor} atoms are significantly "bent back" from the Ir-Me unit. This arrangement is a consequence of the ligand constraints, that is, the "too-short" C–N bonds, which enable strong back donation. Further evidence for this view was provided by the Walsh diagram of the CF_3 substituted diimine model compound, [{2,6-[$C(CF_3)$=$NH]_2$pyridine}IrMe] (Figure 3) bearing a stronger π-acceptor ligand. This situatiuon leads to a preference for the bent over the square-planar structure with a calculated minimum at $\alpha =$ 154°. Finally, this rationale also serves to explain the larger barrier for the bending process in the aforementioned triphosphorus donor complex. Inspection of the DFT optimized structure revealed that the σ* phosphorus π-acceptor orbitals are located in close proximity to the d_{xz} nodal plane and thus, significantly less stabilization through back donation can be achieved.

We have presented a novel thermal C–H activation system and have traced the low activation energies by DFT methods, sterically less crowded complexes are predicted to display even lower C–H activation barriers.

Received: August 8, 2002
Revised: December 30, 2002 [Z19908]

Keywords: C–H bond activation · density functional theory · iridium · N ligands

[1] S. Nückel, P. Burger, *Organometallics* **2001**, *20*, 4345 – 4359.
[2] B. A. Arndtsen, R. G. Bergman, T. A. Mobley, T. H. Peterson, *Acc. Chem. Res.* **1995**, *28*, 154 – 162, and references therein.
[3] R. G. Bergman, *J. Organomet. Chem.* **1990**, *400*, 273 – 282, and references therein.
[4] R. H. Crabtree, *J. Chem. Soc. Dalton Trans.* **2001**, 2437 – 2450.
[5] C. L. Hill, *Activation and Functionalization of Alkanes*, Wiley-Interscience, New York, **1989**, and references therein.
[6] A. E. Shilov, G. B. Shul'pin, *Chem. Rev.* **1997**, *97*, 2879 – 2932, and references therein.
[7] G. A. Luinstra, J. A. Labinger, J. E. Bercaw, *J. Am. Chem. Soc.* **1993**, *115*, 3004 – 3005.
[8] P. L. Watson, *J. Am. Chem. Soc.* **1983**, *105*, 6491 – 6493.
[9] A. Sen, *Acc. Chem. Res.* **1998**, *31*, 550 – 557.
[10] R. A. Periana, D. J. Taube, S. Gamble, H. Taube, T. Satoh, H. Fujii, *Science* **1998**, *280*, 560 – 564.
[11] R. A. Periana, D. J. Taube, E. R. Evitt, D. G. Loffler, P. R. Wentrcek, G. Voss, T. Masuda, *Science* **1993**, *259*, 340 – 343.
[12] W. W. Xu, G. P. Rosini, M. Gupta, C. M. Jensen, W. C. Kaska, K. Krogh-Jespersen, A. S. Goldman, *Chem. Commun.* **1997**, 2273 – 2274.
[13] M. Kanzelberger, B. Singh, M. Czerw, K. Krogh-Jespersen, A. S. Goldman, *J. Am. Chem. Soc.* **2000**, *122*, 11017 – 11018.
[14] R. H. Crabtree, *The Organometallic Chemistry of the Transition Metals*, Wiley-Interscience, New York, **2001**.
[15] S. E. Bromberg, H. Yang, M. C. Asplund, T. Lian, B. K. McNamara, K. T. Kotz, J. S. Yeston, M. Wilkens, H. Frei, R. G. Bergman, C. B. Harris, *Science* **1997**, *278*, 260 – 263.
[16] B. A. Arndtsen, R. G. Bergman, *Science* **1995**, *270*, 1970 – 1973.
[17] Data collection: Stoe IPDS Image Plate System, absorption corrections were carried out numerically. Structure solution: Direct methods using the SHELXS-97 program package; refinement against F^2 with SHELXL-97.[38] All non-hydrogen atoms were refined anisotropically; the position of the hydrogen atoms were calculated in idealized positions and refined using a riding model. Complex **1**: Green needle ($0.37 \times 0.11 \times 0.09$ mm). Orthorhombic cell, space group $P2_12_12_1$ (No. 19), $Z = 4$, $a = 12.914(1)$, $b = 13.021(1)$, $c = 14.0217(8)$ Å, $V = 2357.8(3)$ Å^3, $\rho_{calcd} = 1.625$ g cm^{-3}. 18190 reflections collected, thereof 4360 independent; 4360 reflections used for structure solution and refinement. The refinement converged at final R values $R(I > 2\sigma(I))$: $R1 = 0.0150$ and $wR2 = 0.0301$ for 278 parameters; GOF 1.01, residual electron density: 0.51, −0.5 e Å^{-3} (Flack X-Parameter −0.030(6) and 1.05(2) for the inverted structure). Complex **2**: The crystals were of low quality (presumably twinned); repeated attempts under varied conditions did not provide better single crystals. Brown rectangular parallelepiped ($0.3 \times 0.3 \times 0.2$ mm); triclinic cell, space group $P\bar{1}$ (No. 2), $Z = 2$ with two independent molecules per unit cell. $a = 10.020(1)$, $b = 14.688(1)$, $c = 18.741(2)$ Å, $\alpha = 85.13(1)°$, $\beta = 89.65(1)°$, $\gamma = 72.31(1)°$. $V = 2617.8(2)$ Å^3, $\rho_{calcd} = 1.628$ g cm^{-3}. 9272 independent reflections used for structure solution and refinement. Final R-values (635 parameters) $R(I > 2\sigma(I))$: $R1 = 0.1156$ and $wR2 = 0.3235$. CCDC-191048 (**1**) CCDC-203880 (**2**) contains the supplementary crystallographic data for this paper. These data can be obtained free of charge via www.ccdc.cam.ac.uk/conts/retrieving.html (or from the Cambridge Crystallographic Data Centre, 12 Union Road, Cambridge CB2 1EZ, UK; fax: (+44) 1223-336-033; or deposit@ccdc.cam.ac.uk).
[18] P. L. Watson, G. W. Parshall, *Acc. Chem. Res.* **1985**, *18*, 51 – 56.
[19] P. L. Watson, *J. Chem. Soc. Chem. Commun.* **1983**, 276 – 277.
[20] S. R. Klei, T. D. Tilley, R. G. Bergman, *J. Am. Chem. Soc.* **2000**, *122*, 1816 – 1817.

[21] S. Q. Niu, M. B. Hall, *J. Am. Chem. Soc.* **1998**, *120*, 6169 – 6170.
[22] P. Burger, R. G. Bergman, *J. Am. Chem. Soc.* **1993**, *115*, 10462 – 10463.
[23] T. M. Gilbert, I. Hristov, T. Ziegler, *Organometallics* **2001**, *20*, 1183 – 1189.
[24] K. Eichkorn, O. Treutler, H. Öhm, M. Häser, R. Ahlrichs, *Chem. Phys. Lett.* **1995**, *242*, 652 – 660.
[25] K. Eichkorn, O. Treutler, H. Öhm, M. Häser, R. Ahlrichs, *Chem. Phys. Lett.* **1995**, *240*, 283 – 289.
[26] R. Ahlrichs, M. Bär, M. Häser, H. Horn, C. Kölmel, *Chem. Phys. Lett.* **1989**, *162*, 165 – 169.
[27] S. Dapprich, I. Komaromi, K. S. Byun, K. Morokuma, M. J. Frisch, *J. Mol. Struct.* **1999**, *462*, 1 – 21.
[28] J. Gao in *Reviews in Computational Chemistry, Vol. 7* (Eds.: D. B. Boyd, K. B. Lipkowitz), Wiley, New York, **1996**.
[29] S. Nückel, Dissertation, Universität Zürich **2002**.
[30] H. Werner, A. Höhn, M. Dziallas, *Angew. Chem.* **1986**, *98*, 1112 – 1114; *Angew. Chem. Int. Ed. Engl.* **1986**, *25*, 1090 – 1092.
[31] All stationary points were characterized by the calculation of second derivatives through the absence (minima) or one imaginary frequency (transition states). Transition-state optimizations were performed with John Baker's OPTIMIZE program, available from Parallel Quantum Solutions, Fayetteville, AR, USA, interfaced with Turbomole.
[32] R. T. Price, R. A. Andersen, E. L. Muetterties, *J. Organomet. Chem.* **1989**, *376*, 407 – 417.
[33] M. Sierka, J. Sauer, *J. Chem. Phys.* **2000**, *112*, 6983 – 6996.
[34] J. Y. Saillard, R. Hoffmann, *J. Am. Chem. Soc.* **1984**, *106*, 2006 – 2026.
[35] T. Ziegler, V. Tschinke, L. Y. Fan, A. D. Becke, *J. Am. Chem. Soc.* **1989**, *111*, 9177 – 9185.
[36] A. Dedieu, A. Strich, *Inorg. Chem.* **1979**, *18*, 2940 – 2943.
[37] S. A. Macgregor, O. Eisenstein, M. K. Whittlesey, R. N. Perutz, *J. Chem. Soc. Dalton Trans.* **1998**, 291 – 300.
[38] G. M. Sheldrick, SHELXL-97, Programs for Crystal Structure Solution and Refinement, Universität Göttingen (Germany) **1997**.

